Nucleation and Growth of Gas Bubbles in Elastomers

A. N. GENT AND D. A. TOMPKINS
Institute of Polymer Science, The University of Akron, Akron, Ohio 44304

(Received 6 September 1968; in final form 3 January 1969)

An experimental study is described of the formation and growth of gas bubbles in crosslinked elastomers. A critical condition for bubble formation is found to hold in most cases: The gas supersaturation pressure must exceed $5G/2$, where G is the shear modulus of the elastomer. The kinetics of bubble growth are shown to be in good accord with a simple diffusion-controlled growth relation for a variety of gases, elastomers, temperatures, and pressures. The number of bubbles depends strongly upon the degree of supersaturation above the critical level. This effect is attributed partly to kinetic factors and partly to the presence initially of internal holes of a range of sizes.

I. INTRODUCTION

Bubbles appear in the interior of rubber blocks under suitable circumstances. For example, when a gas is dissolved in the rubber under a sufficiently high pressure and the pressure is then released, the gas will come out of solution internally as bubbles.[1] With high initial pressures, i.e., using highly supersaturated conditions, many small bubbles are formed and the material becomes a closed-cell rubber foam. An experimental study of this process of bubble formation has been carried out and is reported here. Three aspects have been examined: (i) the critical conditions required for any bubble to form, (ii) the dependence of the number of bubbles formed upon the experimental conditions, and, (iii) the rate of growth of an isolated bubble.

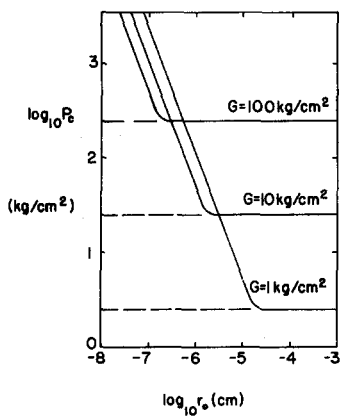

FIG. 1. Critical pressure P_c vs initial hole radius r_0.

The elastomers used in the experiments were crosslinked to different degrees to give a range of hardness. They were all soft rubbery materials, however, with values of shear modulus in the range 1.8–10.0 kg/cm². Three different gases were employed (argon, nitrogen, and carbon dioxide) with a wide range of initial pressure.

Some theoretical considerations are given in the following section. The treatment of the critical conditions for bubble formation differs from conventional nucleation theory by assuming that small holes are present initially in the rubber, and also by assuming that the energy of elastic deformation of the rubber around the hole must be taken into account, in addition to surface energy.[2] As the rubbers were crosslinked, i.e., they were coherent elastic solids, the formation of visible bubbles indicates that local fracture has occurred. It is assumed that the fracture occurred *after* a large elastic expansion and that the energy required for it was much smaller than that required to achieve the initial expansion. Lindsey[3] has attributed the entire resistance to cavitation in a somewhat similar internal fracture phenomenon to a large "surface energy," discussed in terms of fracture energies. In contrast, the present treatment neglects the energy of fracture in comparison with the known elastic energy of inflation and the real (liquid-like) surface energy of the bubble.

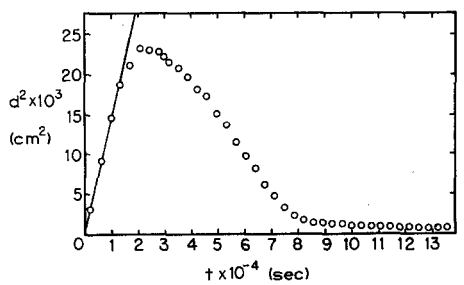

FIG. 2. Bubble diameter d vs time t after release of external pressure. SBR2, argon (P_0=22 kg/cm²), 25°C.

II. THEORETICAL CONSIDERATIONS

Inflation of an initially present small spherical hole is assumed to be resisted by elastic forces and surface tension forces in the rubber. The relation between the pressure P inside the hole and the radius r is then given by[2]

$$P/G=\tfrac{5}{2}-2(r_0/r)-\tfrac{1}{2}(r_0/r)^4+(2\gamma/Gr), \qquad (1)$$

where G is the shear modulus of the rubber (assumed to be Neo-Hookean in elastic behavior), r_0 is the radius of the hole at the time of crosslinking, and γ is the surface energy of the rubber. The value of γ is

[1] Hycar Technical Newsletter Vol. 5, B. F. Goodrich Chemical Company, Cleveland, Ohio, December 1956.

[2] A. N. Gent and D. A. Tompkins (unpublished).

[3] G. H. Lindsey, J. Appl. Phys. **38**, 4843 (1967).

assumed to be similar to that for simple liquids; a value of 25 erg/cm² is adopted for the numerical comparisons given below.

According to Eq. (1) when the initial radius r_0 of the hole is less than γ/G, the pressure P passes through a maximum and then decreases as the radius r increases further. When the initial radius r_0 is greater than γ/G the pressure approaches asymptotically a limiting value of $5G/2$ as the radius increases indefinitely. Thus in both cases there exists a critical value of the internal pressure P_c which is sufficient to cause the hole to expand to an infinite size, the value depending upon the initial size of the hole. Values of P_c are plotted against the initial radius r_0 in Fig. 1, using logarithmic scales for both axes. The values of P_c are seen to be extremely large for small holes, having radii in the range 1–10 Å, but they approach the lower limit of $5G/2$ for holes of the order of 10^{-5} cm initial radius, still well below the visible range.

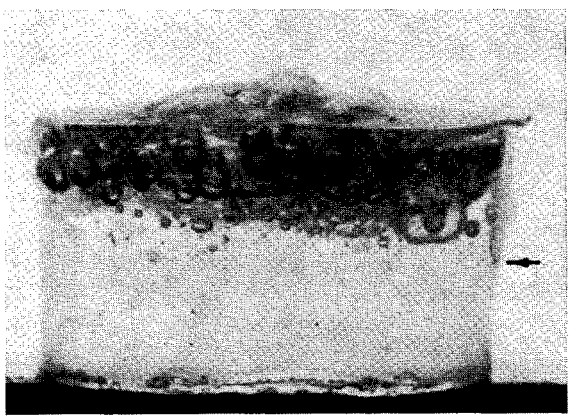

FIG. 3. Cross section of pressure gradient test piece; original magnification ×5, shown here ×1.7; IR1, carbon dioxide (P_1 = 13 kg/cm², P_2 = 1 kg/cm²), 25°C.

The minimum supersaturation pressure for a dissolved gas to form a visible bubble is assumed to be the lower limit for P_c, i.e., $5G/2$. In other words, it is assumed that holes exist of the order of 10^{-5} cm or larger in radius, either in the form of submicroscopic bubbles of air trapped in processing the rubber before crosslinking or in the form of badly wetted particles of dirt or dust. Such holes will be filled by gas when gas dissolves in the rubber, and the gas pressure will inflate them when the external pressure is released. The pressure will be partly maintained during inflation by diffusion of gas into the cavity from the surrounding supersaturated rubber. The kinetics of expansion are discussed below. It should first be noted, however, that a supersaturation pressure greater than the minimum value will be necessary to inflate holes of smaller initial size, less than 10^{-5} cm in radius, in accordance with Fig. 1.

The holes will not expand indefinitely in practice, for two reasons. First, the supply of gas is limited, due to the limited solubility. Second, in blocks of finite size diffusion of gas outwards through the edges of the block is competitive with diffusion into the cavity and eventually provides a means of relieving the supersaturation pressure altogether. The holes thus collapse back to a closed configuration in the end. A typical course of hole expansion and later collapse is shown in Fig. 2. Only the early stages of growth as a visible bubble are considered here, the block being assumed to be infinitely large in comparison with the bubble.

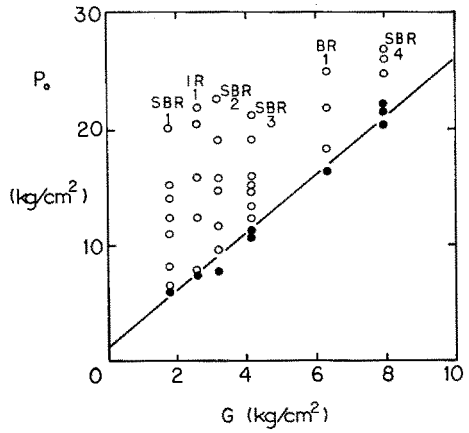

FIG. 4. Cavitation results for SBR, BR, and IR materials. Open circles: visible bubbles formed. Filled-in circles: no bubbles formed. Carbon dioxide, 25°C.

The pressure inside the hole initially will be the same as the initial supersaturation pressure P_0. When the external pressure is released it will drop in accordance with the increased volume as the hole expands, but it will be partly maintained by inward diffusion. We assume that it remains constant during the major part of the visible expansion process at the minimum critical value P_c, given by $5G/2$. The kinetics of growth under these circumstances may be obtained from Epstein and Plesset's relation for the solution of gas bubbles in

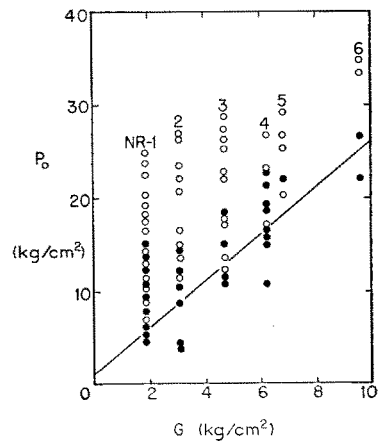

FIG. 5. Cavitation results for NR materials. Open circles: visible bubbles formed. Filled-in circles: no bubbles formed. Carbon dioxide, 25°C.

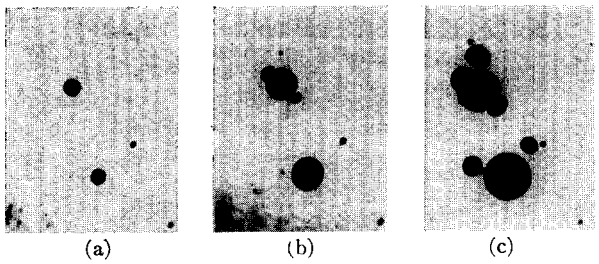

FIG. 6. Bubble growth sequence; original magnification ×35, shown here ×11.9 IR1, argon (P_0=24 kg/cm²), 35°C. (a) 1 min after pressure release, (b) 3 min, and (c) 6 min.

liquids[4] in the form

$$dr/dt = DS'[(P_0/P_c)-1][r^{-1}+(\pi Dt)^{-1/2}], \quad (2)$$

where D is the coefficient of diffusion, S' is the gas solubility under 1 atm pressure in ml at STP per ml of rubber, and r is the radius of the bubble at time t.

The exact solution to Eq. (2) is complex[4,5] but an approximately equivalent relation is given by[4]

$$r = kt^{1/2}, \quad (3)$$

where

$$k = 2(\pi D)^{1/2}\gamma[\gamma+(1+\gamma^2)^{1/2}] \quad (4)$$

and

$$\gamma^2 = S'[(P_0/P_c)-1]/2\pi.$$

Thus the radius of the hole is predicted to increase approximately in proportion to $t^{1/2}$, the rate constant k increasing with D, S', and P_0.

III. EXPERIMENTAL PROCEDURE

A. Test Materials and Properties

Rubber mixes were prepared with the recipes given in the Appendix. They were then vulcanized in the form of sheets 2 to 6 mm thick using the vulcanization conditions given in the Appendix. The products were quite transparent, so that the formation and growth of internal bubbles could be studied. Values of the shear modulus G, given by one-third of Young's modulus, were obtained from tensile stress–strain relations at small extensions and are given in the Appendix, together with values of the coefficients of diffusion D and solubility S' for the gases used in the bubble growth experiments. These were determined from measurements of steady-state gas permeation and the time delay in achieving it, using rubber sheets about 1 mm thick.[6,7] They are in reasonable agreement with previously published values, where these exist.[8]

It is noteworthy that the values of D are quite similar for the three gases whereas the values of S' differ widely. Also the values of D increase strongly with temperature whereas the values of S' do not vary much. Thus the relative importance of D and S' in bubble growth kinetics may be assessed by comparing the effects of different gases (changes in S') with the effects of temperature changes (changes in D). Both properties were found to be involved, as shown later.

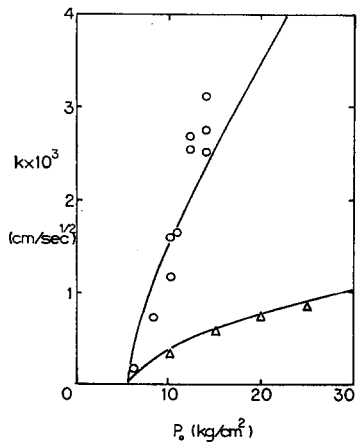

FIG. 8. Growth rate k for material SBR1 vs initial gas pressure P_0. ○, carbon dioxide, 20°C; △, argon, 20°C.

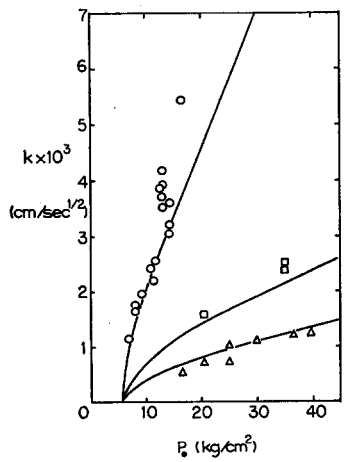

FIG. 7. Growth rate k for material NR1 vs initial gas pressure P_0. ○, carbon dioxide, 25°C; □, nitrogen, 50°C; △, argon, 10°C.

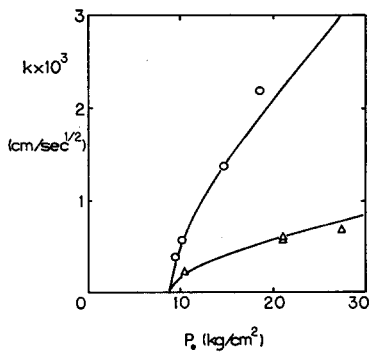

FIG. 9. Growth rate k for material SBR2 vs initial gas pressure P_0. ○, carbon dioxide, 20°C; △, argon, 25°C.

[4] P. S. Epstein and M. S. Plesset, J. Chem. Phys. **18**, 1507 (1950).
[5] I. M. Krieger, G. W. Mulholland, and C. S. Dickey, J. Phys. Chem. **71**, 1123 (1967).
[6] H. A. Daynes, Proc. Roy. Soc. (London) **A97**, 286 (1920).
[7] R. M. Barrer, Trans. Faraday Soc. **35**, 628, 644 (1939).
[8] G. J. van Amerongen, Rubber Chem. Technol. **37**, 1065 (1964).

B. Determination of Bubble Growth Rates

Test pieces in the form of blocks having dimensions of 2.5×2.5×0.6 cm were placed in a pressure cell equipped with glass windows for viewing and recording by time-lapse photography the development of internal bubbles. The cell was first evacuated for 15 min and then pressurized with the particular gas being used for 48 h to allow equilibrium conditions to be attained. The gas pressure (P_0) was held constant during this period and then released by opening a valve. The subsequent development of visible bubbles was recorded photographically using a low power microscope with a 35 mm camera attached, focused on the central plane of the test piece. Magnification of the film allowed bubbles to be observed and measured with a precision of about 10^{-3} cm. Bubbles which appeared near the faces of the test piece were regarded as unrepresentative, and ignored.

C. Determination of Critical Conditions for Bubble Formation

The initial pressure P_0 used in the bubble growth studies was successively reduced until no visible bubbles appeared. In this way an estimate of the minimum pressure P_c was obtained. In addition, an experimental arrangement was developed to secure a pressure gradient through a single test piece. One side of a block about 1.6 cm thick was maintained at a constant pressure P_1 and the opposite side at a constant pressure P_2 for a period of one week, to allow equilibrium conditions to be attained. It was assumed that the internal pressure of dissolved gas then varied linearly with distance through the test piece. The pressures P_1 and P_2 were then released and the distance from the low-pressure face at which cavities appeared was measured (Fig. 3). The corresponding initial pressure was calculated from the assumed linear relationship between pressure and distance.

IV. EXPERIMENTAL RESULTS

A. Critical Conditions for Bubble Formation

The results of experiments using different pressures of carbon dioxide are shown in Figs. 4 and 5. For the butadiene and butadiene-styrene elastomers (Fig. 4) a close correlation was found to hold between the pressure necessary to cause visible bubbles to form and the shear modulus G of the rubber. The full line in Fig. 4 corresponds to the theoretical relation $P_c=5G/2$. It is seen to describe the observations quite accurately. Thus the critical conditions for bubble formation are in accord with the theory in its simplest form, i.e., assuming holes larger than about 10^{-5} cm in radius to be present initially. For the natural rubber vulcanizates the *lowest* gas pressures at which bubbles formed were also in good agreement with the same relation. In many instances, however, no bubbles appeared at substantially higher pressures (Fig. 5). The reason for this is not clear. It may reflect a different distribution of initial hole sizes, with radii of 10^{-5} cm or larger being sometimes absent. When the pressure gradient method was employed to determine the minimum pressure for bubble formation it yielded results in good agreement with theory for the natural rubber materials. The test piece size in this case was much larger, of course, and this may increase the chance of larger holes being present initially.

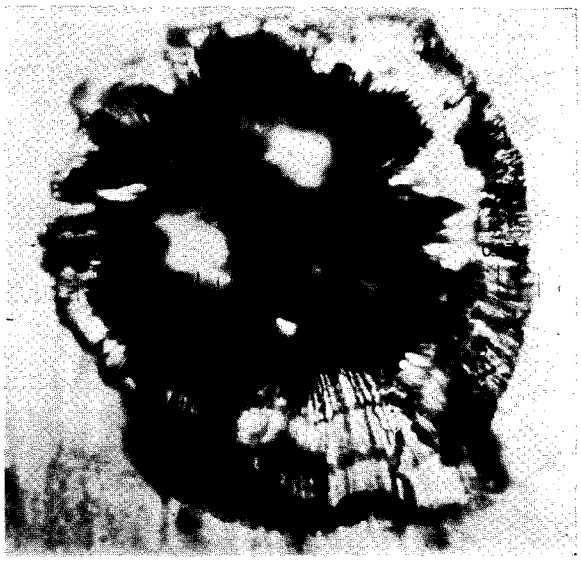

FIG. 11. Bubble cross section after collapse; original magnification ×500, shown here ×200; SBR2, carbon dioxide (P_0 about 14 kg/cm²), 25°C.

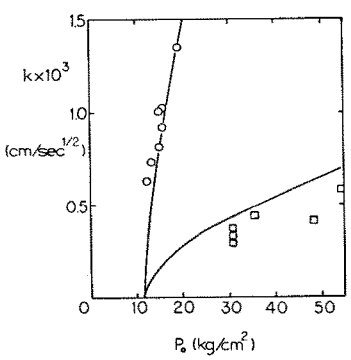

FIG. 10. Growth rate k for material SBR3 vs initial gas pressure P_0. ○, carbon dioxide, 20°C; □, nitrogen, 25°C.

B. Growth Rates

A typical growth sequence is shown in Fig. 6. Bubbles appeared soon after pressure release and then grew as spheres, the radius increasing approximately in proportion to $t^{1/2}$ in the early stages (Fig. 2) in accordance with Eq. (3). The proportionality constant k is used here as a measure of growth rate. Values were determined for several combinations of gas and elastomer and at various temperatures. Some representative results are plotted in Figs. 7–10 against the initial gas pressure P_0. The full curves shown in Figs. 7–10 were

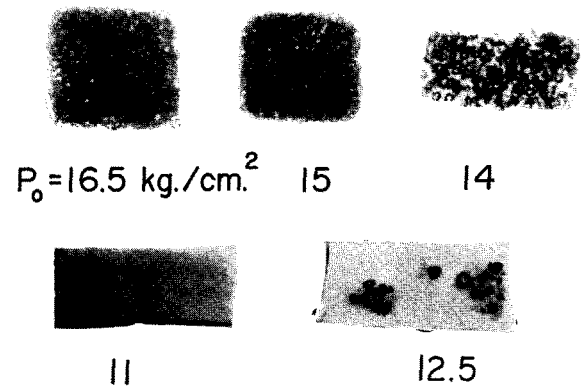

FIG. 12. Test pieces of NR1 using various initial pressures P_0 of carbon dioxide; original magnification about $\times 1$, shown here $\times 0.44$.

calculated from Eq. (4), using the measured values of D and S' and the theoretical value of P_c $(=5G/2)$. They are seen to describe the experimental values of the growth rate k with considerable success in all cases. Thus values of k which correspond to large variations in D, S', P_0, and P_c are all in good accord with a simple diffusion-controlled growth process [Eqs. (2)–(4)] the internal pressure being assumed constant at the value P_c.

For the less-soluble gases, argon and nitrogen, an initial pressure P_0 considerably higher than P_c was necessary to obtain reasonably large rates of growth. At pressures close to P_c no visible bubbles formed. Thus experimental estimates of P_c could not be obtained directly with these gases. Instead, the validity of the theoretical values was inferred from the agreement between the calculated and observed growth rate relations shown in Figs. 7–10.

Several other features of the growth process are noteworthy. First, satellite bubbles often formed in the vicinity of a growing bubble (Fig. 6) and third and fourth generation bubbles were observed in some instances. This phenomenon is attributed to deformation of the material around a bubble, causing a reduction in the critical pressure required for new bubbles to form. Experiments dealing with bubble formation in samples held in a state of simple extension have also been carried out.[2] They showed that the critical pressure P_c is greatly reduced by stretching, in rough accord with a simple theoretical treatment.

Second, in the more highly crosslinked elastomers SBR4 and NR6 the growing cavities did not resemble spherical bubbles but consisted of cracks or circular slits. This is attributed to the low breaking extensions of these materials. The growth kinetics were not examined.

Even for highly extensible materials the appearance of a visible bubble means that internal rupture has taken place. A photomicrograph of a bubble in a cut surface is shown in Fig. 11. Radiating fracture lines can be seen in the surface of the collapsed bubble.

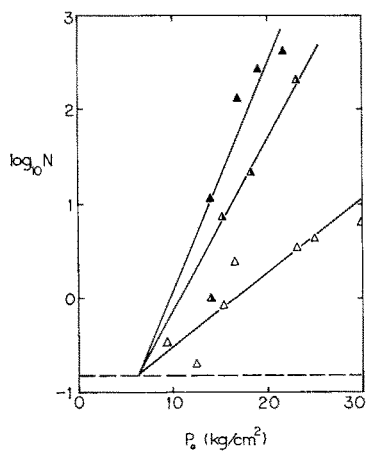

FIG. 13. Number N of primary bubbles per cc vs initial pressure P_0. NR1, argon. △, 10°C; ▲, 35°C; ▲, 65°C. The broken line corresponds to one bubble in the whole test piece.

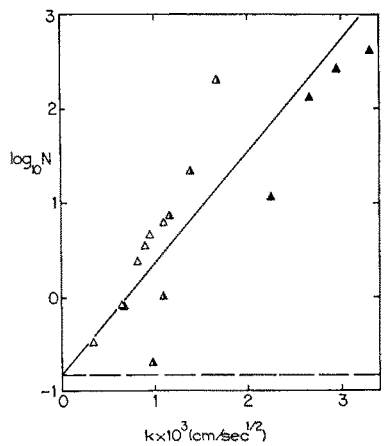

FIG. 14. Number N of primary bubbles per cc vs growth rate k. Data for N taken from Fig. 13.

C. Number of Bubbles Formed

Large numbers of bubbles formed at pressures somewhat higher than P_c (Fig. 12), so that it became difficult to distinguish primary from satellite bubbles and thus to measure accurately the number N of primary bubble sites per unit volume. (Indeed, measurement of the growth rate k was only feasible in the early stages of bubble growth before the proximity of other bubbles distorted the growth behavior or prevented further observation.) Approximate values for N are plotted in Fig. 13 against the initial gas pressure P_0. It might at first be supposed that initial holes of smaller size are activated at higher pressures, in accordance with Fig. 1, so that a larger number of bubbles is formed for this reason. However, it is unlikely that the critical conditions are affected merely by altering the temperature of the experiment, whereas the number of bubbles formed increased markedly at higher temperatures (Fig. 13). It thus seems likely that kinetic factors also affect the number of bubbles formed. Indeed, a strong correlation was found to hold between the number of primary bubbles N and their rate of growth k, as shown in Fig. 14, probably reflecting a common

dependence upon the rate of gas diffusion. Until this effect is understood it is not possible to deduce the distribution of hole sizes present initially from the observed number of gas bubbles formed at various initial pressures.

V. General Conclusions

The theoretical treatment adequately describes the initial rates of growth of visible gas bubbles for various elastomer–gas combinations and at various temperatures and pressures. Since it does not involve any arbitrary parameters, it may be regarded as quite satisfactory. The critical conditions for *any* visible bubble to form are in good agreement with the theory, taking into account only the elastic energy of inflation of an initially present hole, i.e., neglecting surface and fracture energies. This is equivalent to assuming that the initial holes are relatively large in size, greater than about 10^{-5} cm in radius. The critical condition is apparently higher in the case of sparingly soluble gases, due mainly to the slow growth of bubbles at low degrees of supersaturation. It is much reduced for stretched samples, as dealt with elsewhere.[2]

At a pressure higher than the critical value the number of bubbles formed should correspond to the number of holes present initially which exceed a certain size. However it is clear from experiments with argon (chosen because the bubbles formed are smaller with this less-soluble gas and hence easier to distinguish) that a kinetic effect is also present. At a constant degree of supersaturation the number of bubbles formed depends upon their rate of growth. Further work is required to clarify this aspect.

ACKNOWLEDGMENTS

This work was supported by a research grant from the National Science Foundation Engineering Division. It was presented at the 2nd International Conference on Cellular Plastics (New York, 6–8 November 1968) organized by the Cellular Plastics Division of the Society of the Plastics Industry. The authors are indebted to the Firestone Tire and Rubber Company, Phillips Petroleum Company, and Shell Chemical Company for supplying elastomers.

APPENDIX: TEST MATERIALS AND PROPERTIES

A. Compound Recipes in Parts by Weight and Vulcanization Conditions

Materials designated NR1–NR6 were prepared from natural rubber (pale crepe) 100, antioxidant (Agerite Spar, Vanderbilt) 1, dicumyl peroxide 0.5, 1, 2, 3, 4, and 6. They were vulcanized for 60 min at 150°C. The material designated IR was prepared using the same recipe and vulcanization conditions as for NR2, except that polyisoprene (310, Shell Chemical Company) was used in place of natural rubber.

Materials designated SBR1–SBR4 were prepared from a butadiene-styrene copolymer (75/25, Solprene 300, Phillips Petroleum Company) 100, antioxidant 1, dicumyl peroxide 1, 2, 3, and 4, sulphur 0.15, 0.3, 0.45, and 0.45, and *N*-cyclohexyl-2-benzthiazyl sulphenamide 0.15, 0.3, 0.45, and 0.45. They were vulcanized for 30 min at 150°C. The material designated BR was prepared using the same recipe and vulcanization conditions as for SBR3, except that polybutadiene (Solprene 200, Phillips Petroleum Company) was used in place of the butadiene-styrene copolymer.

B. Shear Modulus G

Material	NR 1	2	3	4	5	6	IR
G (kg/cm²)	1.9	3.1	4.7	6.2	6.8	9.6	2.6

Material	SBR 1	2	3	4	BR
G (kg/cm²)	1.8	3.2	4.2	8.0	6.3

C. Coefficients of Diffusion D and Solubility S' for Carbon Dioxide at 20°–25°C

Material	NR1	NR2	NR3	SBR1	SBR2	SBR3
$D\times10^6$ (cm²/sec)	1.75	1.45	1.25	0.75	0.80	0.75
S'	0.60	0.95	0.75	0.95	0.85	1.0

D. Coefficients of Diffusion D and Solubility S' for Different Gases at Different Temperatures

Temperature	10°C	23°C	35°C	50°C
	$D\times10^6$ (cm²/sec) for material NR2			
Carbon dioxide	...	1.45	...	4.35
Nitrogen	...	1.10	...	...
Argon	0.60	1.35	2.30	4.40
	S' for material NR2			
Carbon dioxide	...	0.95	...	0.70
Nitrogen	...	0.06	...	...
Argon	0.14	0.11	0.13	0.11

Temperature	20°C	30°C	40°C	50°C
	$D\times10^6$ (cm²/sec) for material SBR2			
Nitrogen	...	0.70	1.1	2.1
Argon	0.50	0.70	1.5	3.1
	S' for material SBR2			
Nitrogen	...	0.07	0.08	0.07
Argon	0.11	0.10	0.11	0.09